Published in final edited form as:
Clin Cancer Res. 2008 September 1; 14(17): 5376–5384. doi:10.1158/1078-0432.CCR-08-0455.

Overexpression of the zinc uptake transporter hZIP1 inhibits NF-κB and reduces the malignant potential of prostate cancer cells *in vitro* and *in vivo*

Konstantin Golovine[1], **Peter Makhov**[1], **Robert G. Uzzo**, **Tavis Shaw**, **David Kunkle**, and **Vladimir M. Kolenko**
Department of Surgical Oncology, Fox Chase Cancer Center, Philadelphia, PA 19111

Abstract

Purpose—Intracellular zinc levels and expression of the zinc uptake transporter, hZIP1, are markedly down-regulated in prostate adenocarcinomatous tissue compared with normal prostate tissue. Our previous studies have demonstrated that zinc inhibits NF-κB activity and reduces the malignant potential of prostate cancer cells *in vitro*. In this study, we investigate the functional impact of hZIP1 overexpression on NF-κB activity and tumorigenic potential in human prostate cancer cells *in vitro* and *in vivo*.

Experimental Design—NF-κB activity in PC-3 prostate cancer cells was examined by Western blotting and luciferase assay. ELISA was used to examine the expression of tumorigenic cytokines. TUNEL, adhesion, and invasiveness assays were used to assess the malignant potential of tumor cells. The impact of hZIP1 overexpression on prostate tumor progression *in vivo* was assessed using a xenograft model.

Results—Overexpression of the hZIP1 transporter in PC-3 cells results in significant inhibition of NF-κB activity in the presence of physiological levels of zinc. NF-κB inhibition coincides with a reduction in expression of several NF-κB controlled pro-metastatic and anti-apoptotic factors as well as sensitization of the cells to etoposide and TRAIL mediated cell death. Moreover, over-expression of the hZIP1 transporter induces regression of prostate tumor growth in a xenograft model.

Conclusions—Our results demonstrate that hZIP1 overexpression has a functional impact on the malignant potential of prostate cancer cells via inhibition of NF-κB-dependent pathways and support the concept that hZIP1 may function as a tumor suppressor gene in prostate cancer.

Keywords

zinc; hZIP1; NF-κB; prostate; cancer

Requests for reprints: Vladimir M. Kolenko, Fox Chase Cancer Center, 333 Cottman Avenue, Philadelphia, PA 19111, USA, Phone: 215-728-5620 Fax: 215-728-4333 E-mail address: Vladimir.Kolenko@fccc.edu.
[1]These authors contributed equally to this work

Statement of clinical relevance

Substantial information exists implicating changes in zinc accumulation in the development and progression of prostatic malignancies. Zinc levels and the expression of zinc uptake transporters, hZIP1 and hZIP2, are down-regulated in malignant cells in situ compared with normal prostate glandular epithelial cells. Moreover, there is a strong association between prostate cancer in African-American men and down-regulation of hZIP1 and hZIP2 transporters. Early response genes related to NF-κB contribute to neoplastic transformation and metastatic tumor progression. Our present study reveals that overexpression of hZIP1 in PC-3 prostate cancer cells reduces the tumorigenic potential of prostate cancer cells via inhibition of NF-κB-dependent pathways. These data may support the development of novel strategies for therapeutic interventions in prostate cancer.

Introduction

The process whereby a normal prostate epithelial cell transforms into a cancerous cell involves the loss of the cells ability to accumulate intracellular zinc (1,2). The loss of zinc accumulation is one of the most consistent and persistent characteristics of prostatic malignancy. Zinc concentrations diminish early in the course of prostate cancer, preceding the initial histopathologic changes of prostate cancer, and continue to decline during the ultimate progression toward hormone-independent growth (3–5). Several investigators have shown that intra-mitochondrial accumulation of high levels of zinc effectively inhibits mitochondrial aconitase activity, which in turn has been shown to inhibit citrate oxidation. This inhibition essentially truncates the Krebs cycle and markedly decreases overall cellular energy production. The energy requirements for malignancy can readily be achieved in cancer cells that have undergone the metabolic transformation towards zinc deficiency via increased citrate-oxidation along with a functional Krebs cycle (1,2). In addition, zinc induces an apoptotic pathway in prostate cells, which results from its direct effect on mitochondrial release of cytochrome c followed by activation of the caspase cascade and ultimately apoptosis (6,7). Other recent studies have demonstrated a correlation between zinc concentration and the ability of androgen-dependent LNCaP prostate cancer cells to invade Matrigel, whereby, invasion of Matrigel is suppressed in the presence of higher zinc concentrations (8) and is associated with the ability of zinc to irreversibly inhibit aminopeptidase N (9).

Although decreased serum zinc concentrations have been reported in patients with metastatic prostate carcinoma (10), this is not likely to be the major cause for decreased zinc accumulation in malignant prostate cells. Specialized mechanisms are required for both zinc uptake and release (11). Zinc transporters are largely assigned to two metal-transporter families: the ZIP family, which imports zinc and the ZnT family which functions in releasing zinc or sequestering zinc internally. To date, 14 mammalian ZIP members have been identified; however, only hZIP1, hZIP2 and hZIP3 have been localized to the plasma membrane (12–16). The expression of the hZIP1 gene and transporter protein is markedly down-regulated in adenocarcinomatous glands and in prostate intra-epithelial neoplastic foci compared with normal peripheral zone glandular epithelium and benign hyperplastic glands (3). Moreover, recent studies reveal a strong association of prostate cancer in African-American men with down-regulation of hZIP1 and hZIP2 transporters (17). PC-3 and RWPE-2 malignant prostate cells overexpressing hZIP1 exhibit increased zinc uptake and have significantly slower growth rates than parental cells (18,19). Therefore, hZIP1 has been proposed to function as a tumor suppressor gene in prostate cancer (20).

Previously we have demonstrated that treatment of prostate cancer cells *in vitro* with physiological levels of zinc in the presence of the zinc ionophore, pyrithione, inhibits NF-κB activity. In turn, inhibition of NF-κB leads to a reduction in the expression of certain NF-κB-regulated pro-angiogenic and pro-metastatic factors, namely, VEGF, IL-6, IL-8, and MMP-9 (21,22). The Rel/NF-κB family of eukaryotic transcription factors is comprised of several structurally related proteins that form homo- and heterodimers. The most common Rel/NF-κB dimer in mammals contains the p50-RelA subunit and is specifically called NF-κB. The activity of NF-κB is regulated by its interaction with inhibitory IκB proteins, which block the ability of NF-κB to enter the nucleus and bind to DNA. Multiple studies have established the role of NF-κB regulated genes in malignant transformation (23), metastatic progression of prostate cancer (24) and resistance to therapeutic regimens (25). NF-κB regulates the susceptibility of various cell types to apoptosis through transcriptional control of anti-apoptotic genes, which act on different levels of the apoptotic pathway (26).

Our present study reveals that overexpression of the zinc uptake transporter, hZIP1 in PC-3 cells results in a significant inhibition of NF-κB activity in the presence of physiological levels

of zinc and reduction of the tumorigenic potential and growth of prostate cancer cells both *in vitro* and *in vivo.*

Materials and Methods

Cells and culture conditions

Androgen-independent human PC-3 prostate cancer cells were obtained from ATCC (Rockville, MD) and cultured in RPMI 1640 (Bio-Whittaker, Walkersville, MD) supplemented with 10% FCS (Hyclone, Logan, UT), gentamicin (50 mg/l), sodium pyruvate (1 mM) and non-essential amino acids (0.1 mM) under conditions indicated in the figure legends. Actual experiments were performed in RPMI 1640 medium.

Antibodies and Reagents

Antibody to actin was obtained from Sigma Corporation (St. Louis, MO). Antibodies to Bcl-X_L, Bcl-2 and XIAP were obtained from Cell Signaling Technology (Beverly, MA). Antibodies to RelA, p50, IκBα and TOPO I were obtained from Santa Cruz Biotechnology (Santa Cruz, CA). Secondary horseradish peroxidase-conjugated donkey anti-rabbit antibodies were purchased from Amersham (Arlington Hts., IL). TRAIL was purchased from Biomol (Plymouth Meeting, PA). Etoposide was obtained from Calbiochem (San Diego, CA). The hZIP1 antibody and CMV-hZIP1 expression vector were kindly provided by Dr. R. Franklin (University of Maryland) and have been described previously (18). FluoZin-3 AM was obtained from Molecular Probes (Eugene, OR).

Stable Transfection of PC-3 cells with hZIP1

To create the hZip1 C-end FLAG-tagged expression vector, hZip1 ORF was obtained by PCR with 5′-atcttg aagctt gcc acc atg gga ccg tgg gga gag cca gag ctc ctg gtg-3′ (forward) and 5′-atcttg tctaga tta att aat cta ctt atc gtc gtc atc ctt gta atc gat ttg gat gaa gag cag gcc-3′ (reverse) primers using pRC-CMV-hZip1vector as a template and then cloned into the HindIII/Xba1 restriction sites of the pRC-CMV plasmid. PC-3 cells were transfected with either the hZIP1 expression vector or the CMV control vector using the TransIT-Prostate transfection kit (Mirus Bio, Madison, WI). Selection was performed using G418 (1.5 mg/mL; Invitrogen/Life Technologies), and screening of clones was based on Western Blot analysis with anti-hZIP1 antibody to determine hZIP1 expression. Stable transfectants were maintained in medium containing G418 (500 μg/mL).

FluoZin-3 staining

Cells were incubated with 1 μg/ml of zinc in the form of $ZnSO_4$ for 1 hour, washed twice with PBS, loaded with 5 μM FluoZin-3 AM at room temperature for 30 min and analyzed by flow cytometry. Analysis was performed using FACScan (Becton Dickinson, Franklin Lakes, NJ). Individual fluorescent populations were determined through the use of acquisition and analysis software (Cell Quest, Becton Dickinson).

Atomic Absorption Spectroscopy

The total zinc concentration of cells, plasma and tumor tissue specimens was measured by flame mode using a Shimadzu AA-6300 atomic absorption spectrophotometer. Cells were incubated with 1.5 μg/ml of zinc in the form of $ZnSO_4$ for 3 hours. Harvested cells were rinsed three times in PBS, digested in 2% SDS and boiled for 10 minutes. Protein concentrations were measured with BCA protein assay (Pierce, Rockford, IL). To examine accumulation of zinc in tumor tissue specimens, portions of the tumor specimens were weighted, homogenized, digested in 2% SDS and boiled for 10 minutes. Zinc levels were re-calculated according to wet

tissue weight. The plasma samples were diluted with 0.1 N nitric acid before the determination of zinc concentration.

Luciferase reporter assay

Cells were transfected with pNF-κB-luc (Stratagene, La Jolla, CA), pRL-TK or pGL3-control-luc (Promega, Madison, WI) plasmids. Twenty-four hours after transfection, cells were treated with 1.5 μg/ml of zinc in the form of $ZnSO_4$ for 3 hours in RPMI medium followed by incubation with 10 ng/ml of TNF-α for an additional 3 hours. Samples were assayed for firefly and renilla luciferase activities using the Dual-Glo Luciferase assay System (Promega) and normalized as instructed by the manufacturer.

Western Blot Analysis

Nuclear and cytoplasmic extracts and whole cell lysates were prepared as described previously (27). Protein concentrations were measured with BCA protein assay reagents (Pierce, Rockford, IL). Equivalent amounts of proteins (20 μg) were mixed with an equal volume of 2X Laemmli sample buffer, boiled and resolved by electrophoresis in 10% sodium dodecyl sulfate-polyacrylamide gels (SDS-PAGE). The proteins were transferred from the gel to a nitrocellulose membrane using an electroblotting apparatus (Bio-Rad) (15 V, 3 mA/cm^2 for 24 minutes). Membranes were then incubated in a blocking solution containing 5% nonfat dry milk overnight to inhibit nonspecific binding. The membranes were then incubated with specific antibody (1–3 μg/ml) for 2 hours. After washing in TRIS/0.1% Tween 20 for 30 minutes, membranes were incubated for another 30 minutes with horseradish peroxidase-conjugated secondary antibody. The membranes were then washed and developed with enhanced chemiluminescence (ECL Western Blotting Kit, Amersham, Arlington Heights, IL).

ELISA

IL-6, IL-8 and VEGF levels in cell culture supernatants and tumor tissue extracts were determined by ELISA kits (R&D Systems, Minneapolis, MN). Tumor tissue specimens were homogenized in 1% Tween 20/PBS containing a proteinase inhibitor cocktail (Roche Applied Science) as previously described (28) and then centrifuged. Protein concentrations were measured with BCA protein assay reagents (Pierce, Rockford).

Measurement of apoptosis

DNA fragmentation was detected using the APO-BRDU kit (The Phoenix Flow Systems, Inc., San Diego, CA) according to the protocols provided with the kit.

Gelatin zymography

The gelatinolytic activity of MMP-9 was determined in the conditioned cell culture supernatants using zymogram gels (Bio-Rad, Hercules, CA) as suggested by the manufacturer.

Immunocytometry

Surface expression of ICAM-1 was determined by staining cells with FITC-conjugated anti-ICAM-1 antibodies (R&D Systems, Minneapolis, MN) for 30 min on ice. Stained cells were washed twice with PBS and analyzed by flow cytometry. Analysis was performed on the FACScan (Becton Dickinson, Franklin Lakes, NJ). Individual fluorescent populations were determined through the use of acquisition and analysis software (Cell Quest, Becton Dickinson).

Adhesion Assay

Cells were stained with Calcein AM (2 μM), pre-incubated with 1.5 μg/ml of zinc in the form of $ZnSO_4$ for 6 hours and plated in triplicates onto 96-well plates (2.5×10^3cells per well) pre-coated with fibronectin (50 μg/ml). Cells were allowed to attach at 37°C for 30 minutes. Wells were then washed with PBS twice and images were captured using a fluorescence microscope equipped with a digital camera.

Analysis of cell invasiveness

Invasiveness was determined using a BD Falcon™ HTS FluoroBlok system (BD Biosciences, Bedford, MA) in triplicate for each condition. Cells (2.5×10^3) were seeded in the upper compartment of the FluoroBlok chamber in the absence of serum with or without 1.5 μg/ml of zinc in the form of $ZnSO_4$. Serum-containing medium in the lower compartment served as a chemoattractant. Cells were incubated at 37°C for 12 hours and then stained with 2μM of Calcein-AM. An intervening membrane was present to block fluorescence from labeled cells present in the top chamber of the insert system. Images have been captured using fluorescence microscope equipped with a digital camera.

Assessment of *in vivo* tumor growth

For *in vivo* studies, 1×10^6 PC-3-hZIP1 or PC-3-CMV cells were inoculated s.c. in the flank region of 6 week old male C.B17/Icr-scid mice using a 27-gauge needle. All animal procedures were done according to local guidelines on animal care and with appropriate institutional certification. Animals were fed an autoclaved AIN-93M diet (Harlan Teklad, Madison, WI) and water *ad libitum*. Dietary zinc supplementation (2000 ppm zinc) was provided by adding $ZnSO_4$ to the drinking water and started one week prior to tumor cell implantation. Tumors were measured twice weekly and their volumes were calculated by the formula: [volume = $0.52 \times (\text{width})^2 \times \text{length}$]. None of the mice showed signs of wasting or other visible indications of toxicity. After 23 days of xenograft implantation animals were sacrificed by CO_2 asphyxiation. At the termination of the experiment, blood was collected from the retro-orbital plexus under anesthesia from both experimental and control groups. Tumor tissue specimens were collected to assess zinc levels, the status of NF-κB activity and VEGF and IL-8 contents. Zinc levels in plasma and tissue samples were examined by Atomic Absorption Spectroscopy.

EMSA and supershift analysis

Isolation of nuclear extracts and EMSA were performed as previously described (29). For supershift assay anti-p50 antibody (Santa Cruz Biotechnology Inc., Santa Cruz, CA) was added to the binding reaction buffer. Incubation continued for 20min at 25°C. Complexes were separated by electrophoresis on a 5% polyacrylamide gel in 1xTAE for 4h at 140V, dried and exposed to HyBlot CL autoradiography film (Denville Scientific) at −80°C.

Statistical analysis

Statistical analysis was performed by ANOVA. Where only two groups are compared, a Student's t-test was applied. Results are expressed as the mean ± SEM. A P-value of <0.05 was considered statistically significant.

Results

Overexpression of hZIP1 transporter results in the inhibition of NF-κB activity in PC-3 prostate cancer cells

Activation of the nuclear transcription factor NF-κB is thought to be a major event contributing to malignant transformation and progression in prostate cancer (23,30,31). We have previously demonstrated that treatment with physiological levels of zinc in the presence of the zinc

ionophore, pyrithione, inhibits NF-κB activity in prostate cancer cells (21,22). Pyrithione was used to facilitate the transport of zinc across the cell membrane of prostate cancer cells since these cells have lost the ability to accumulate zinc. Recent studies demonstrate that prostate cancer cells overexpressing the hZIP1 transporter exhibit increased zinc uptake compared with parental cells (18,19). To investigate whether overexpression of the zinc uptake transporter, hZIP1 has a functional impact on the status of NF-κB activity in prostate cancer cells, we generated PC-3 cells with stable overexpression of hZIP1 (Fig. 1A). Zinc uptake was examined in parental PC-3 cells and cells transfected with either hZIP1 (PC-3-hZIP1) or the CMV control vector (PC-3-CMV). Consistent with the ability of hZIP1 to enhance intracellular zinc uptake (13), accumulation of liable (Fig. 1B) and total (Fig. 1C) zinc levels were significantly increased in PC-3-hZIP1 cells cultured in the presence of physiologically relevant concentrations of zinc (a reference interval for the serum zinc level is 0.5–1.5 μg/ml (32)) as was determined by staining cells with the cell permeable zinc specific fluorescent indicator, Fluo-Zin-3 followed by FACS analysis, and atomic absorption spectrophotometry respectively. Importantly, although notable fractions of parental and PC-3-CMV cells were positively stained with Fluo-Zin-3 after incubation with zinc, the intensity of staining was significantly lower in control cells than in hZIP1 transfectants given the logarithmic scale of the X axis representing fluorescence intensity.

To investigate whether increased zinc uptake in PC-3-hZIP1 cells has a functional impact on the status of NF-κB activity, PC-3-hZIP1 and PC-3-CMV cells were cultured with and without zinc followed by stimulation with TNF-α. The findings presented in Figure 2A demonstrate that zinc supplementation completely blocked TNF-α-induced degradation of the inhibitory subunit IκBα in PC-3-hZIP1 cells but not in PC-3-CMV cells. Nuclear extracts from the same samples were subjected to SDS-PAGE followed by Western Blotting with anti-RelA or p50 antibodies. In PC-3-hZIP1 cells incubated with zinc, the lack of IκBα degradation correlated with complete inhibition of nuclear accumulation of both RelA and p50 proteins (Fig. 2A). In contrast, zinc supplementation failed to prevent nuclear translocation of RelA and p50 in PC-3-CMV cells. To further explore the impact of hZIP1 overexpression on the NF-κB transcriptional activity, we performed an NF-κB-dependent luciferase *cis*-reporter assay. Cells were cultured with and without zinc at 1.5 μg/ml followed by stimulation with TNF-α. The findings presented in Figure 2B demonstrate that TNF-αinduced NF-κB transcriptional activity was significantly reduced in PC-3-hZIP1 but not in PC-3-CMV cells. In contrast, the addition of zinc had no impact on the expression of the SV40-driven pGL3-luc control construct (Fig. 2B).

Levels of tumorigenic cytokines, IL-6 and IL-8, and activity of MMP-9 are reduced in PC-3 cells overexpressing hZIP1

The progressive growth and metastasis of prostate cancer is mediated by the secretion of various NF-κB-controlled tumorigenic cytokines, including IL-6, IL-8 and MMP-9 (30,33). Expression of these molecules by prostate cancer cells has been shown to correlate with malignant potential (34,35). To investigate the potential impact of hZIP1 overexpression on the production of tumorigenic cytokines, we examined the expression of IL-6 and IL-8 cytokines in the cell culture supernatants of PC-3-hZIP1 and PC-3-CMV cells in the presence of physiologically relevant level of zinc. As shown in Figure 2C, supernatants collected from PC-3-hZIP1 cells cultured in the presence of 1.5 μg/ml of zinc showed a significantly decreased amount of secreted IL-6 and IL-8 when compared with supernatants obtained from control PC-3-CMV cells.

In addition, we examined MMP-9 enzymatic activities using conditioned medium from PC-3-hZIP1 and PC-3-CMV cells cultured with and without zinc followed by stimulation with TNF-

α. Decrease in MMP-9 activity measured by gelatin zymography was clearly observed in PC-3-hZIP1 cells conditioned medium (Fig. 2D).

Functional impact of hZIP1 overexpression on the invasive and adhesive properties of prostate cancer cells

Recent studies demonstrate that NF-κB also regulates expression of the intercellular adhesion molecule-1 (ICAM-1) (36,37). Increased expression of ICAM-1 correlates with an increased metastatic potential of prostate cancer cells (34,38). Given our findings of a zinc inhibitory effect on NF-κB activation, we examined whether zinc supplementation also decreases expression of ICAM-1 on the surface of PC-3-hZIP1 cells. Immunostaining with anti-ICAM-1 antibody revealed that the addition of zinc to the cell culture medium notably inhibits TNF-α-mediated ICAM-1 up-regulation on PC-3-hZIP1 but not in PC-3-CMV cells (Fig. 3A). We hypothesized that zinc-mediated inhibition of NF-κB activity in PC-3-hZIP1 cells would have a functional impact on their metastatic potential. Indeed, zinc supplementation produced a notable inhibitory effect on the adhesion of PC-3-hZIP1 to a fibronectin-coated plate (Fig. 3B). Next, we examined the effect of zinc on cell invasiveness since adhesion and migration are interrelated processes responsible for the invasion and metastasis of cancer cells. The findings presented in Figure 3C demonstrate that reduced adhesive potential of hZIP1 transfectants coincide with a significantly lower invasion rate. Together, these results suggest that increased expression of the hZIP1 transporter may have a functional impact on tumorigenic potential of prostate cancer cells.

hZIP1 overexpression results in the reduced expression of anti-apoptotic Bcl-2, Bcl-X_L and XIAP proteins and sensitization of PC-3 prostate cancer cells to cytotoxic agents

NF-κB regulates expression of numerous genes with known anti-apoptotic activity and inhibition of NF-κB sensitizes prostate cancer cells to various cytotoxic agents (22,39). Given our findings of an inhibitory effect of zinc on the NF-κB activity, we examined whether increased intracellular zinc uptake also has an impact on the expression of NF-κB-regulated anti-apoptotic proteins. The data presented in Figure 4A demonstrates that in the PC-3-hZIP1 cells supplemented with zinc at 1.5 μg/ml, the expression of the NF-κB-controlled anti-apoptotic proteins, Bcl-2, Bcl-X_L and XIAP are significantly reduced in comparison with the control PC-3-CMV cells. Next, we examined the functional impact of hZIP1 overexpression on the sensitivity of PC-3 cells to cytotoxic agents using the TUNEL assay. Treatment with etoposide induced negligible levels of apoptosis in both cell lines while treatment with TRAIL alone induced apoptosis in 21.4% and 23.5% of PC-3-CMV and PC-3-hZIP1 cells respectively. Supplementation of cell culture medium with zinc also failed to induce significant levels of cell death in both cell lines. However, simultaneous addition of zinc and either etoposide or TRAIL resulted in profound DNA fragmentation in PC-3-hZIP1 cells whereas no increase in apoptotic cell death was observed in PC-3-CMV (Figure 4B). These results suggest that down-regulation of anti-apoptotic proteins in hZIP1 overexpressing cells exposed to physiological levels of zinc may contribute, at least in part, to the sensitization of prostate cancer cells to drug mediated apoptosis.

Overexpression of hZIP1 suppresses growth of prostate tumor xenografts in a mouse model

The *in vivo* effect of the zinc-enriched diet on growth of PC-3-hZIP1 and PC-3-CMV cells was evaluated in the xenograft mouse model. Dietary zinc supplementation started one week prior to tumor cell implantation. PC-3-hZIP1 and PC-3-CMV xenograft tumors were established in 6 weeks old male C.B17/Icr-scid mice. After 23 days of tumor cells implantation zinc supplementation decreased tumor volume from 400 mm^3 to 174 mm^3 (P=0.036) in animals with PC-3-hZIP1 tumors (Fig. 5A). Zinc supplementation also caused an observable, but not statistically significant, decrease in growth of tumors established from PC-3-CMV cells (528

mm^3 vs. 438 mm^3, P=0.310) (Fig. 5A). During the course of this study, no mouse suffered any untoward toxicity from the zinc supplementation, and none of the mice died.

Zinc levels in the plasma and tumor specimens were measured to validate zinc availability and its uptake by PC-3-hZIP1 and PC-3-CMV cells. Findings presented in Figure 5B demonstrate that plasma zinc concentration was significantly increased in mice fed a zinc-supplemented diet compared with mice fed the control diet. In contrast, zinc levels in tumor tissue specimens were significantly increased in mice fed zinc-supplemented diet and injected with PC-3-hZIP1 but not PC-3-CMV cells (Fig. 5C).

To determine the effect of dietary zinc supplementation on NF-κB activation in prostate cancer xenografts, EMSA was performed. NF-κB inhibition was not detected in the tumor specimens of animals with PC-3-CMV xenografts fed zinc-supplemented diet. On the contrary, notable decrease of NF-κB activity in the PC-3-hZIP1 xenografts of mice on the zinc-supplemented diet was revealed (Fig. 6A). We also carried out supershift assays to demonstrate that the observed bands are specific for NF-κB. Reaction mixtures were incubated in the presence or absence of the anti-p50 antibody and subjected to electrophoresis. Figure 6A shows the supershifted nucleoprotein complex only in samples pre-incubated with anti-p50 antibody.

Furthermore, we also found that the decrease of NF-κB activity coincided with the reduced VEGF and IL-8 contents in tumors (Fig. 6B). Together, these findings demonstrate that zinc supplementation was able to effectively inhibit NF-κB activation in hZIP1 overexpressing prostate tumors *in vivo*.

Discussion

Several reports suggest that the decreased zinc level in malignant prostate tissue is not entirely due to a decreased availability of zinc in the circulation (1,14). The ability of prostate cells to accumulate zinc is regulated by the expression and activity of the zinc uptake transporters, including the major zinc uptake transporter, hZIP1 (18). To avoid the anti-tumor effects of zinc, malignant prostate cells exhibit a silencing of the expression of the hZIP1 gene accompanied by a depletion of cellular zinc (40). hZIP1 has therefore been proposed to function as a tumor suppressor gene in prostate cancer (20). Increased constitutive activation of NF-κB in prostate cancer cells is believed to be a major event contributing to malignant transformation and progression of the prostate cancer phenotype (30,41). We have demonstrated previously that treatment with physiological levels of zinc in the presence of the zinc ionophore, pyrithione, effectively inhibits NF-κB activity and functionally suppresses the malignant potential of prostate cancer cells (21,22). Results of our current experiments clearly demonstrate that overexpression of the zinc uptake transporter hZIP1 in human PC-3 prostate cancer cells leads to a prominent inhibition of NF-κB activity in the presence of physiologically acceptable levels of zinc. The inhibition of NF-κB in turn reduces the tumorogenic potential both *in vitro* and *in vivo.*

The molecular mechanisms underlying prostate tumor progression are not completely understood. However, there is growing evidence that the progressive growth of prostate cancer is mediated by the secretion of various NF-κB-controlled tumorigenic cytokines, including IL-6, IL-8, VEGF and MMP-9 (30,33). In this study we hypothesized that increased zinc uptake would abolish the expression of certain NF-κB-regulated genes in hZIP1 transfectants secondary to the inhibitory effects of zinc on NF-κB activity. Indeed, the levels of secreted IL-6 and IL-8 were significantly lower in PC-3-hZIP1 compared with control PC-3-CMV cells. The results of these experiments corroborate with previously published observation that NF-κB signaling blockade is sufficient to inhibit expression of pro-angiogenic molecules and therefore potentially decrease neoplastic angiogenesis (30).

It is important to note that in our experiments NF-κB inhibition was observed at zinc concentrations that had no significant direct effect on cell death rate. These results indicate that suppression of NF-κB by zinc is not simply a byproduct of the molecular events triggered by the cell death process but rather it is a direct and independent effect of zinc. Here, we also report that overexpression of hZIP1 transporters promotes down-regulation of the NF-κB-controlled anti-apoptotic proteins, Bcl-2 and Bcl-X_L in PC-3 cells. Multiple studies document that overexpression of anti-apoptotic proteins controlled by NF-κB have been implicated as a key element of drug resistance in a wide variety of tumors (25,42). Indeed, overexpression of anti-apoptotic Bcl-2 family proteins play an important role in the aggressive behavior of prostate cancer cells and their resistance to cytotoxic agents (43). XIAP acts as inhibitor of apoptosis induced by both extrinsic and intrinsic apoptosis pathways and is often overexpressed in human malignancies (44). Taken together, these findings make the XIAP and Bcl-2 family of proteins prominent targets for therapeutic intervention. Our experiments show that reduced expression of Bcl-2, Bcl-X_L and XIAP in hZIP1 overexpressing PC-3 cells coincides with an increased apoptotic susceptibility of these cells to TRAIL and etoposide, which induce apoptosis by intrinsic and extrinsic pathways, respectively (45). Importantly, these results were obtained by supplementing cells with physiologically relevant levels of zinc. In addition, the presented data are in agreement with the results of others demonstrating that zinc exerts a direct effect on mitochondria and promotes pore-forming process for release of cytochrome c. Indeed, recombinant Bcl-2 and Bcl-X_L are capable of preventing mitochondrial permeability transition pore opening in cells and isolated mitochondria (46). Thus, results of our experiments could explain at least in part a mitochondrial apoptogenic effect of zinc.

One critical aspect of our study was to examine whether overexpression of hZIP1 in PC-3 cells is able to increase zinc uptake sufficiently to inhibit growth of prostate tumor cells *in vivo*. In animals fed a zinc-enriched diet the zinc levels in tumor xenografts established from PC-3-hZIP1 cells were significantly higher compared with zinc levels in tumor tissue specimens obtained from animals with PC-3-CMV tumors. Notably, the increased zinc accumulation in PC-3-hZIP1 tumors was associated with inhibition of tumor growth, decreased levels of NF-κB activity and reduced VEGF and IL-8 contents.

Taken together, these data provide strong evidence that the loss or silencing of the major zinc uptake transporter hZIP1 may be an important factor in the development and progression of prostate cancer supporting the concept that hZIP1 may function as a tumor suppressor gene in prostate cancer.

Acknowledgements

This work was supported by National Institutes of Health Grant RO1 CA108890 (VMK).

References

1. Costello LC, Franklin RB. Novel role of zinc in the regulation of prostate citrate metabolism and its implications in prostate cancer. Prostate 1998;35:285–96. [PubMed: 9609552]
2. Costello LC, Franklin RB. The intermediary metabolism of the prostate: a key to understanding the pathogenesis and progression of prostate malignancy. Oncology 2000;59:269–82. [PubMed: 11096338]
3. Franklin RB, Feng P, Milon B, et al. hZIP1 zinc uptake transporter down regulation and zinc depletion in prostate cancer. Mol Cancer 2005;4:32. [PubMed: 16153295]
4. Ogunlewe JO, Osegbe DN. Zinc and cadmium concentrations in indigenous blacks with normal, hypertrophic, and malignant prostate. Cancer 1989;63:1388–92. [PubMed: 2465818]
5. Zaichick V, Sviridova TV, Zaichick SV. Zinc in the human prostate gland: normal, hyperplastic and cancerous. Int Urol Nephrol 1997;29:565–74. [PubMed: 9413764]

6. Feng P, Li TL, Guan ZX, Franklin RB, Costello LC. Direct effect of zinc on mitochondrial apoptogenesis in prostate cells. Prostate 2002;52:311–8. [PubMed: 12210492]
7. Feng P, Liang JY, Li TL, et al. Zinc induces mitochondria apoptogenesis in prostate cells. Mol Urol 2000;4:31–6. [PubMed: 10851304]
8. Ishii K, Otsuka T, Iguchi K, et al. Evidence that the prostate-specific antigen (PSA)/Zn2+ axis may play a role in human prostate cancer cell invasion. Cancer Lett 2004;207:79–87. [PubMed: 15050736]
9. Ishii K, Usui S, Sugimura Y, et al. Aminopeptidase N regulated by zinc in human prostate participates in tumor cell invasion. Int J Cancer 2001;92:49–54. [PubMed: 11279605]
10. Feustel A, Wennrich R, Schmidt B. Serum-Zn-levels in prostatic cancer. Urol Res 1989;17:41–2. [PubMed: 2922890]
11. McMahon RJ, Cousins RJ. Regulation of the zinc transporter ZnT-1 by dietary zinc. Proc Natl Acad Sci U S A 1998;95:4841–6. [PubMed: 9560190]
12. Gaither LA, Eide DJ. The human ZIP1 transporter mediates zinc uptake in human K562 erythroleukemia cells. J Biol Chem 2001;276:22258–64. [PubMed: 11301334]
13. Gaither LA, Eide DJ. Functional expression of the human hZIP2 zinc transporter. J Biol Chem 2000;275:5560–4. [PubMed: 10681536]
14. Costello LC, Liu Y, Zou J, Franklin RB. Evidence for a zinc uptake transporter in human prostate cancer cells which is regulated by prolactin and testosterone. J Biol Chem 1999;274:17499–504. [PubMed: 10364181]
15. Kambe T, Yamaguchi-Iwai Y, Sasaki R, Nagao M. Overview of mammalian zinc transporters. Cell Mol Life Sci 2004;61:49–68. [PubMed: 14704853]
16. Eide DJ. The SLC39 family of metal ion transporters. Pflugers Arch 2004;447:796–800. [PubMed: 12748861]
17. Rishi I, Baidouri H, Abbasi JA, et al. Prostate cancer in African American men is associated with downregulation of zinc transporters. Appl Immunohistochem Mol Morphol 2003;11:253–60. [PubMed: 12966353]
18. Franklin RB, Ma J, Zou J, et al. Human ZIP1 is a major zinc uptake transporter for the accumulation of zinc in prostate cells. J Inorg Biochem 2003;96:435–42. [PubMed: 12888280]
19. Huang L, Kirschke CP, Zhang Y. Decreased intracellular zinc in human tumorigenic prostate epithelial cells: a possible role in prostate cancer progression. Cancer Cell Int 2006;6:10. [PubMed: 16579854]
20. Costello LC, Franklin RB. The clinical relevance of the metabolism of prostate cancer; zinc and tumor suppression: connecting the dots. Mol Cancer 2006;5:17. [PubMed: 16700911]
21. Uzzo RG, Crispen P, Golovine K, Makhov P, Horwitz E, Kolenko VM. Diverse effects of zinc on NF-kB and AP-1 transcription factors: Implications for prostate cancer progression. Carcinogenesis. 2006
22. Uzzo RG, Leavis P, Hatch W, et al. Zinc Inhibits Nuclear Factor-kappaB Activation and Sensitizes Prostate Cancer Cells to Cytotoxic Agents. Clin Cancer Res 2002;8:3579–83. [PubMed: 12429649]
23. Hsu TC, Nair R, Tulsian P, et al. Transformation nonresponsive cells owe their resistance to lack of p65/nuclear factor-kappaB activation. Cancer Res 2001;61:4160–8. [PubMed: 11358840]
24. Luo JL, Tan W, Ricono JM, et al. Nuclear cytokine-activated IKKalpha controls prostate cancer metastasis by repressing Maspin. Nature. 2007
25. Lashinger LM, Zhu K, Williams SA, Shrader M, Dinney CP, McConkey DJ. Bortezomib abolishes tumor necrosis factor-related apoptosis-inducing ligand resistance via a p21-dependent mechanism in human bladder and prostate cancer cells. Cancer Res 2005;65:4902–8. [PubMed: 15930312]
26. Dutta J, Fan Y, Gupta N, Fan G, Gelinas C. Current insights into the regulation of programmed cell death by NF-kappaB. Oncogene 2006;25:6800–16. [PubMed: 17072329]
27. Kolenko V, Bloom T, Rayman P, Bukowski R, Hsi E, Finke J. Inhibition of NF-kappa B activity in human T lymphocytes induces caspase-dependent apoptosis without detectable activation of caspase-1 and -3. J Immunol 1999;163:590–8. [PubMed: 10395645]
28. Lu S, Lee J, Revelo M, Wang X, Lu S, Dong Z. Smad3 is overexpressed in advanced human prostate cancer and necessary for progressive growth of prostate cancer cells in nude mice. Clin Cancer Res 2007;13:5692–702. [PubMed: 17908958]

29. Wu L, Pu Z, Feng J, Li G, Zheng Z, Shen W. The ubiquitin-proteasome pathway and enhanced activity of NF-kappaB in gastric carcinoma. J Surg Oncol. 2007
30. Huang S, Pettaway CA, Uehara H, Bucana CD, Fidler IJ. Blockade of NF-kappaB activity in human prostate cancer cells is associated with suppression of angiogenesis, invasion, and metastasis. Oncogene 2001;20:4188–97. [PubMed: 11464285]
31. Sweeney C, Li L, Shanmugam R, et al. Nuclear factor-kappaB is constitutively activated in prostate cancer in vitro and is overexpressed in prostatic intraepithelial neoplasia and adenocarcinoma of the prostate. Clin Cancer Res 2004;10:5501–7. [PubMed: 15328189]
32. Henry, J. Clinical Diagnosis and Management by Laboratory Methods. 19. Philadelphia, PA: WB Saunders Co; 1996.
33. Chung TD, Yu JJ, Spiotto MT, Bartkowski M, Simons JW. Characterization of the role of IL-6 in the progression of prostate cancer. Prostate 1999;38:199–207. [PubMed: 10068344]
34. Aalinkeel R, Nair MP, Sufrin G, et al. Gene expression of angiogenic factors correlates with metastatic potential of prostate cancer cells. Cancer Res 2004;64:5311–21. [PubMed: 15289337]
35. Ferrer FA, Miller LJ, Andrawis RI, et al. Angiogenesis and prostate cancer: in vivo and in vitro expression of angiogenesis factors by prostate cancer cells. Urology 1998;51:161–7. [PubMed: 9457313]
36. Tozawa K, Sakurada S, Kohri K, Okamoto T. Effects of anti-nuclear factor kappa B reagents in blocking adhesion of human cancer cells to vascular endothelial cells. Cancer Res 1995;55:4162–7. [PubMed: 7545088]
37. Farina AR, Cappabianca L, Mackay AR, et al. Transcriptional regulation of intercellular adhesion molecule 1 by phorbol ester in human neuroblastoma cell line SK-N-SH involves jun-and fos-containing activator protein 1 site binding complex(es). Cell Growth Differ 1997;8:789–800. [PubMed: 9218873]
38. Gho YS, Kim PN, Li HC, Elkin M, Kleinman HK. Stimulation of tumor growth by human soluble intercellular adhesion molecule-1. Cancer Res 2001;61:4253–7. [PubMed: 11358852]
39. Coffey RN, Watson RW, O'Neill AJ, Mc Eleny K, Fitzpatrick JM. Androgen-mediated resistance to apoptosis. Prostate 2002;53:300–9. [PubMed: 12430141]
40. Franklin RB, Costello LC. Zinc as an anti-tumor agent in prostate cancer and in other cancers. Arch Biochem Biophys 2007;463:211–7. [PubMed: 17400177]
41. Suh J, Payvandi F, Edelstein LC, et al. Mechanisms of constitutive NF-kappaB activation in human prostate cancer cells. Prostate 2002;52:183–200. [PubMed: 12111695]
42. Tu Y, Renner S, Xu F, et al. BCL-X expression in multiple myeloma: possible indicator of chemoresistance. Cancer Res 1998;58:256–62. [PubMed: 9443402]
43. Papadopoulos K. Targeting the Bcl-2 family in cancer therapy. Semin Oncol 2006;33:449–56. [PubMed: 16890799]
44. Schimmer AD, Dalili S, Batey RA, Riedl SJ. Targeting XIAP for the treatment of malignancy. Cell Death Differ 2006;13:179–88. [PubMed: 16322751]
45. Sun XM, MacFarlane M, Zhuang J, Wolf BB, Green DR, Cohen GM. Distinct caspase cascades are initiated in receptor-mediated and chemical-induced apoptosis. J Biol Chem 1999;274:5053–60. [PubMed: 9988752]
46. Kroemer G. Mitochondrial control of apoptosis: an overview. Biochem Soc Symp 1999;66:1–15. [PubMed: 10989652]

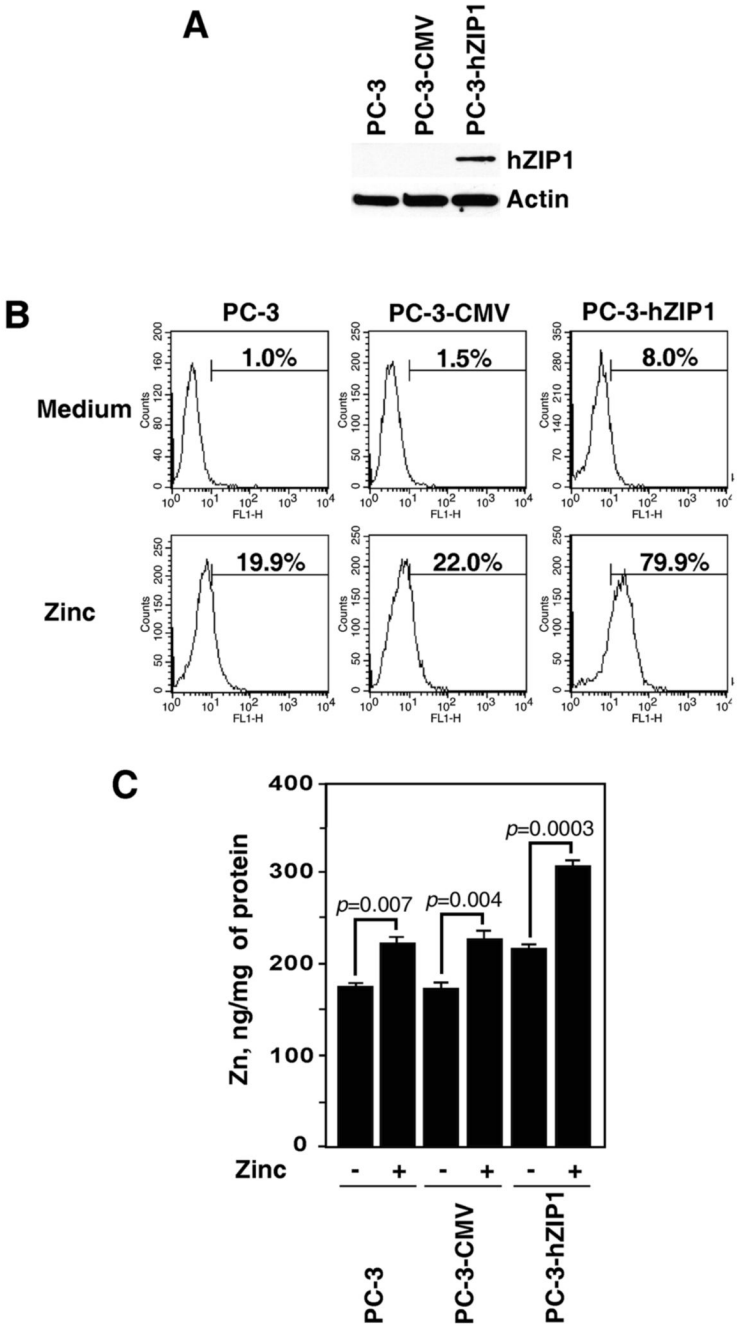

Figure 1.

Over-expression of the hZIP1 transporter increases liable and total levels of zinc in PC-3 prostate cancer cells. (A) Western blot analysis of hZIP1 expression in parental PC-3 cells and cells stably transfected with either hZIP1 or the CMV control vectors. (B) Accumulation of liable zinc in parental and hZIP1 transfected PC-3 cells. X axis represents fluorescence intensity, Y axis represents cell number. The numbers represent the percentage of cells in populations positively stained with FluoZin-3. Representative data from one of five experiments. (C) Total zinc levels in parental and hZIP1 transfected PC-3 cells. Zinc levels were examined as described in Materials and Methods. Columns, means of four different experiments; bars, SEM.

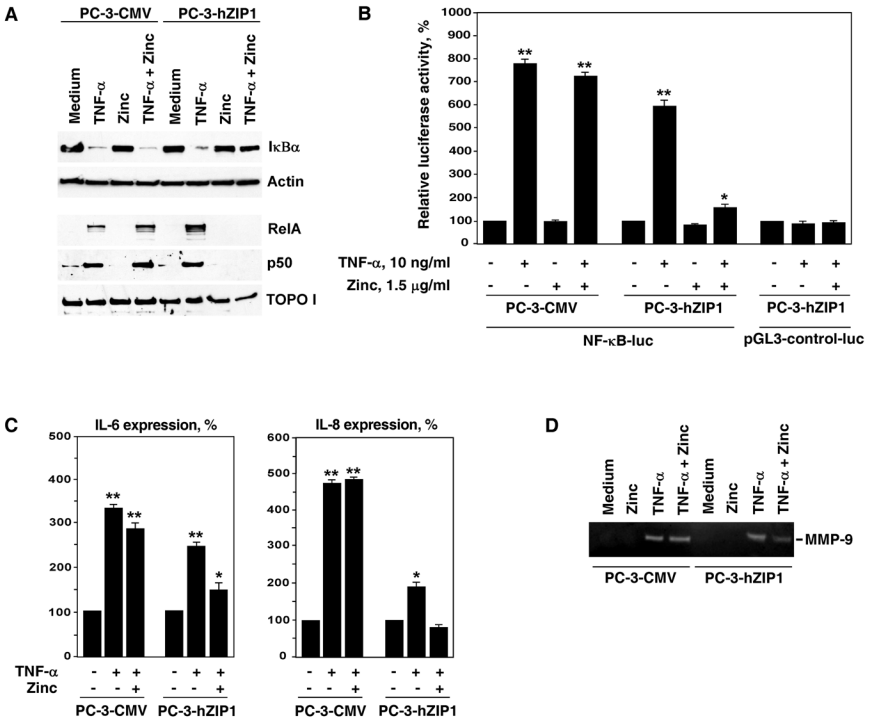

Figure 2.

Physiological levels of zinc inhibit NF-κB activation and suppress expression of pro-tumorigenic cytokines in PC-3 cells overexpressing the hZIP1 transporter. (A) RelA and p50 proteins levels in nuclear extracts of PC-3 cells transfected with either hZIP1 or the CMV control vectors. Cells were pre-incubated with 1.5 μg/ml of zinc in the form of $ZnSO_4$ for 3 hours followed by incubation with 10 ng/ml of TNF-α for 30 minutes. RelA and p50 proteins levels were determined by Western blot analysis with specific antibodies. Expression of TOPO I was used to control equal protein loading in nuclear extracts. Cytoplasmic extracts from the same samples were subjected to SDS-PAGE followed by Western Blot analysis with anti-IκBα antibody. Expression of actin was used to control equal protein loading in cytoplasmic extracts. Representative data from one of three experiments. (B) Luciferase reporter assay of NF-κB activity in PC-3 cells transfected with hZIP1 or the CMV control vectors. Luciferase activity of the NF-κB-independent SV40-driven pGL3-control-luc vector was used as a control. Luciferase assay was performed as described in Materials and Methods. Columns, means of three different experiments; bars, SEM. *$P < 0.05$, **$P < 0.01$ compared with cells cultured in medium alone. (C) PC-3 cells transfected with either hZIP1 or the CMV control vectors were pre-incubated with 1.5 μg/ml of zinc in the form of $ZnSO_4$ in triplicates for 3 hours followed by stimulation with 10 ng/ml TNF-α for 18 hours. IL-6 and IL-8 levels in cell culture supernatants were determined by ELISA as described in Materials and Methods. Columns, means of three different experiments; bars, SEM. *$P < 0.05$, **$P < 0.01$ compared with cells cultured in medium alone. (D) Control and experimental cells were treated as described above. Gelatinolytic activity of MMP-9 in cell culture supernatants was determined as described in Materials and Methods. Representative data from one of three experiments.

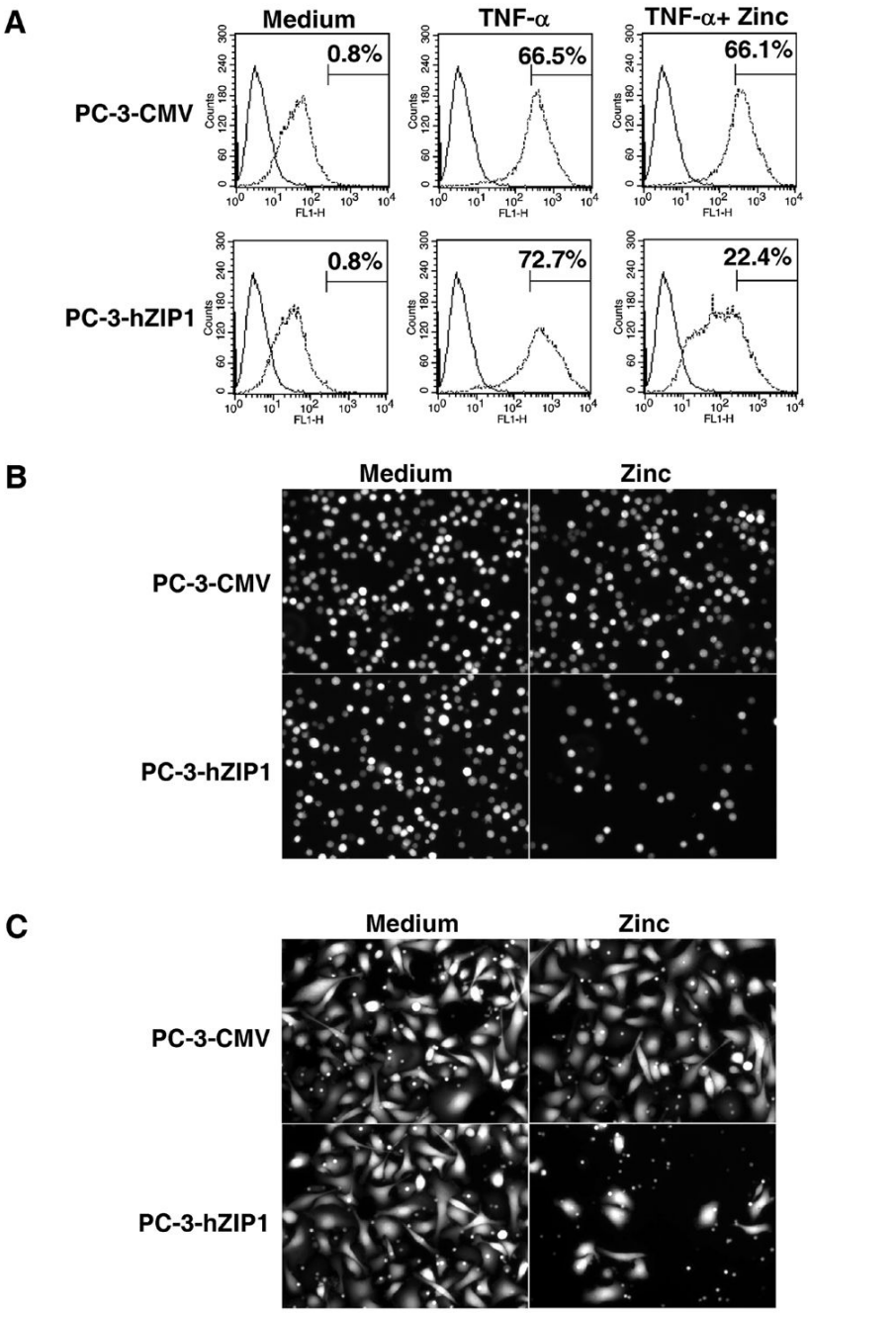

Figure 3.

(A) Cell surface expression of ICAM-1 in hZIP1 transfectants and control cells. Cells were pre-incubated with 1.5 μg/ml of zinc for 3 hours followed by stimulation with 10 ng/ml TNF-α for 12 hours. Analysis of ICAM-1 expression was performed as described in Materials and Methods. Matched isotypic control was used for a particular subclass of Ig and system employed (solid line). X axis represents fluorescence intensity; y axis represents cell number. Numbers represent the percentage of cells in populations positively stained for ICAM-1. Representative data from one of three experiments. (B) Effect of hZIP1 over-expression on the adhesion of PC-3 cells. Representative images of attached cells from one of four experiments.

(C) Effect of hZIP1 over-expression on the invasiveness of PC-3 cells. Representative images of cells invaded through the membrane from one of three experiments.

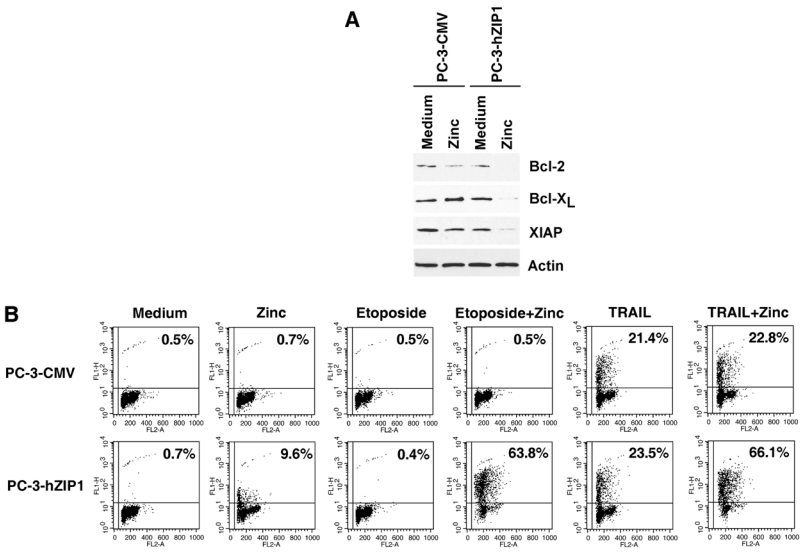

Figure 4.

(A) Expression of NF-κB-regulated anti-apoptotic proteins in hZIP1 transfectants and control cells. Cells were incubated with 1.5 μg/ml of zinc in the form of $ZnSO_4$ for 18 hours. Cell lysates were subjected to SDS-PAGE, blotted, and probed with antibodies as indicated. Expression of actin was used to control equal protein loading. (B) Over-expression of hZIP1 sensitizes PC-3 cells to etoposide and TRAIL mediated apoptosis. PC-3 cells were pre-incubated with 1.5 μg/ml of zinc for 3 hours followed by treatment with etoposide (50 μg/ml) or TRAIL (250 ng/ml) for 18 hours. The percentage of apoptotic cells was determined by APO-BRDU assay followed by flow cytometry analysis as indicated in Materials and Methods. X axis represents DNA content; Y axis represents fluorescence intensity. Representative data from one of four experiments.

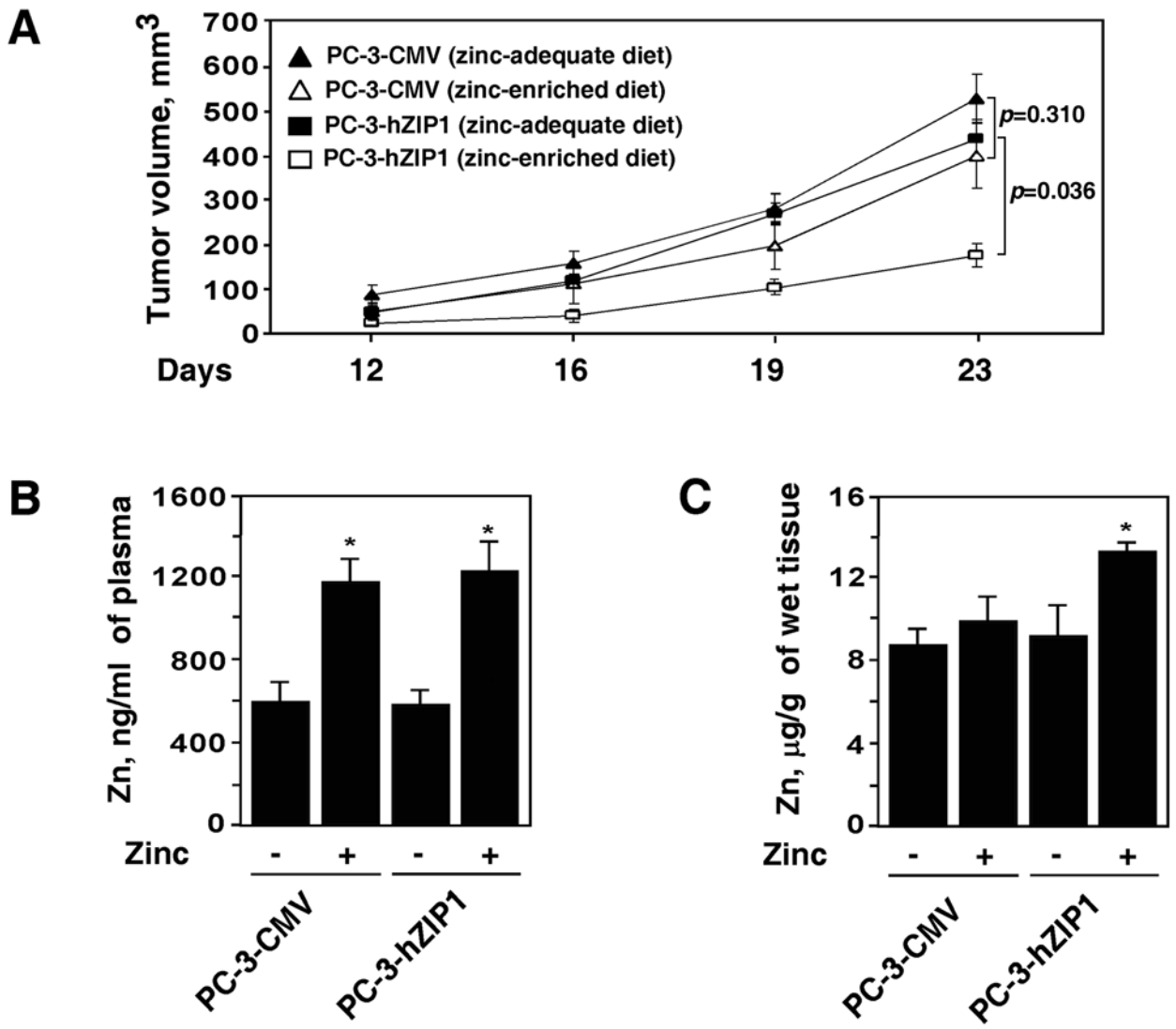

Figure 5.

(A) The effect of hZIP1 over-expression on prostate tumor growth *in vivo*. PC-3-hZIP1 (squares) or PC-3-CMV (triangles) cells were inoculated s.c. in the flank region of 6 week old male C.B17/Icr-scid mice. Animals were maintained on a zinc-adequate (filled symbols) or on a zinc-enriched (open symbols) AIN-93M diet. Tumor volumes were measured as described in Materials and Methods. (B) Plasma zinc concentration in the experimental and control groups of animals. (C) Zinc levels in tumor tissue specimens obtained from the experimental and control groups of animals. Data shown in A-C are mean values of 5 mice in each group; bars, SEM. **P* < 0.05 compared with the zinc-adequate diet.

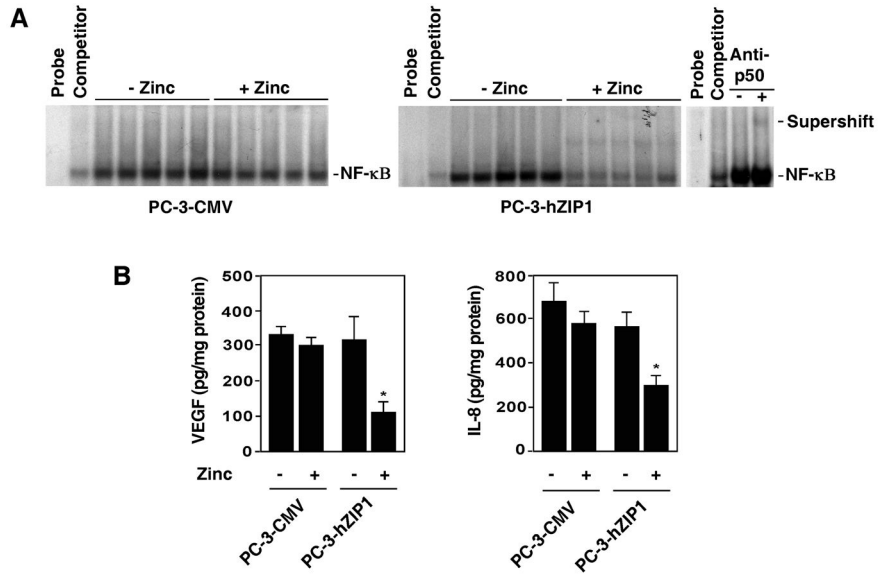

Figure 6.

(A) Zinc supplementation inhibits NF-κB DNA binding activity in hZIP1 over-expressing prostate tumors *in vivo*. NF-κB activity was examined by EMSA in nuclear extracts prepared from control and hZIP1 overexpressing tumors as described in Materials and Methods. Supershift analysis using p50 antibody was performed to confirm that the observed bands are specific for NF-κB. (B) VEGF and IL-8 contents in tumors. The amount of VEGF and IL-8 was measured by ELISA as described in the Materials and Methods. Data shown in B are mean values of 5 tumor specimens in each group; bars, SEM. **P* < 0.05 compared with the zinc-adequate diet.